Integrated Design of Working Fluid Mixtures and Absorption Refrigeration Cycles

Athanasios I. Papadopoulos[1]*, Alexios-Spyridon Kyriakides[1], Panos Seferlis[1,2] and Ibrahim Hassan[3]

[1]Chemical Process and Energy Resources Institute (CPERI), Centre for Research and Technology Hellas (CERTH), Thessaloniki, Greece, [2]Department of Mechanical Engineering, Aristotle University of Thessaloniki, Thessaloniki, Greece, [3]Mechanical Engineering Department, Texas A&M University at Qatar, Doha, Qatar

This work presents a CAMD (computer-aided molecular design) approach for the design of working fluid mixtures used in ABR (absorption refrigeration) cycles. Compared to previous works, the proposed approach introduces two major improvements. It employs for the first time an ABR process model in the course of CAMD, hence enabling the evaluation of the generated mixtures considering process performance indicators. It enables for the first time the simultaneous generation and evaluation of molecular structures for both refrigerants and absorbents. The employed model and CAMD optimization problem formulation incorporates major ABR operational driving forces pertaining to efficient refrigeration, sufficient solubility of mixture components and ease of separation in the generator. The approach employs a multicriteria assessment methodology both during CAMD and for the evaluation of selected mixtures using a more rigorous ABR model at a second stage. The work identifies novel mixtures, with Acetaldehyde/2-Methoxyethyl acetate and Acetaldehyde/Methanediol exhibiting the highest performance. The latter exhibits 3% higher COP (coefficient of performance) and cooling output than the reference mixture NH_3/H_2O, whereas it operates at 87 and 89% lower high and low cycle pressures. The novel mixtures are also compared with novel mixtures previously identified through a heuristic approach by the authors. The latter mixtures indicate overall higher ABR performance but similar or worse performance in safety, health and environmental impact indices. Further performance improvements may be achieved by including into CAMD additional chemical groups to be able to simulate the complex absorbent structures available in published works.

Keywords: molecular design, absorption refrigeration, multicriteria assessment, working fluids, CAMD

INTRODUCTION

Absorption refrigeration (ABR) is an important technology for the transformation of heat into cooling (Best and Rivera, 2015). A feature that makes it appealing is that it is able to exploit heat sources within a wide temperature range, from low-grade, renewable (Shirazi et al., 2018), and waste heat (Kale et al., 2018) to cleaner hydrocarbon fuels, such as natural gas (Azhar and Siddiqui, 2019). The operation of ABR is relatively simple as it is based on the use of a binary working fluid which undergoes various phase changes to produce cooling in common and simple heat exchangers. Compared to conventional, energy intensive vapor compression systems, ABR requires an insignificant amount of energy to pump a liquid phase.
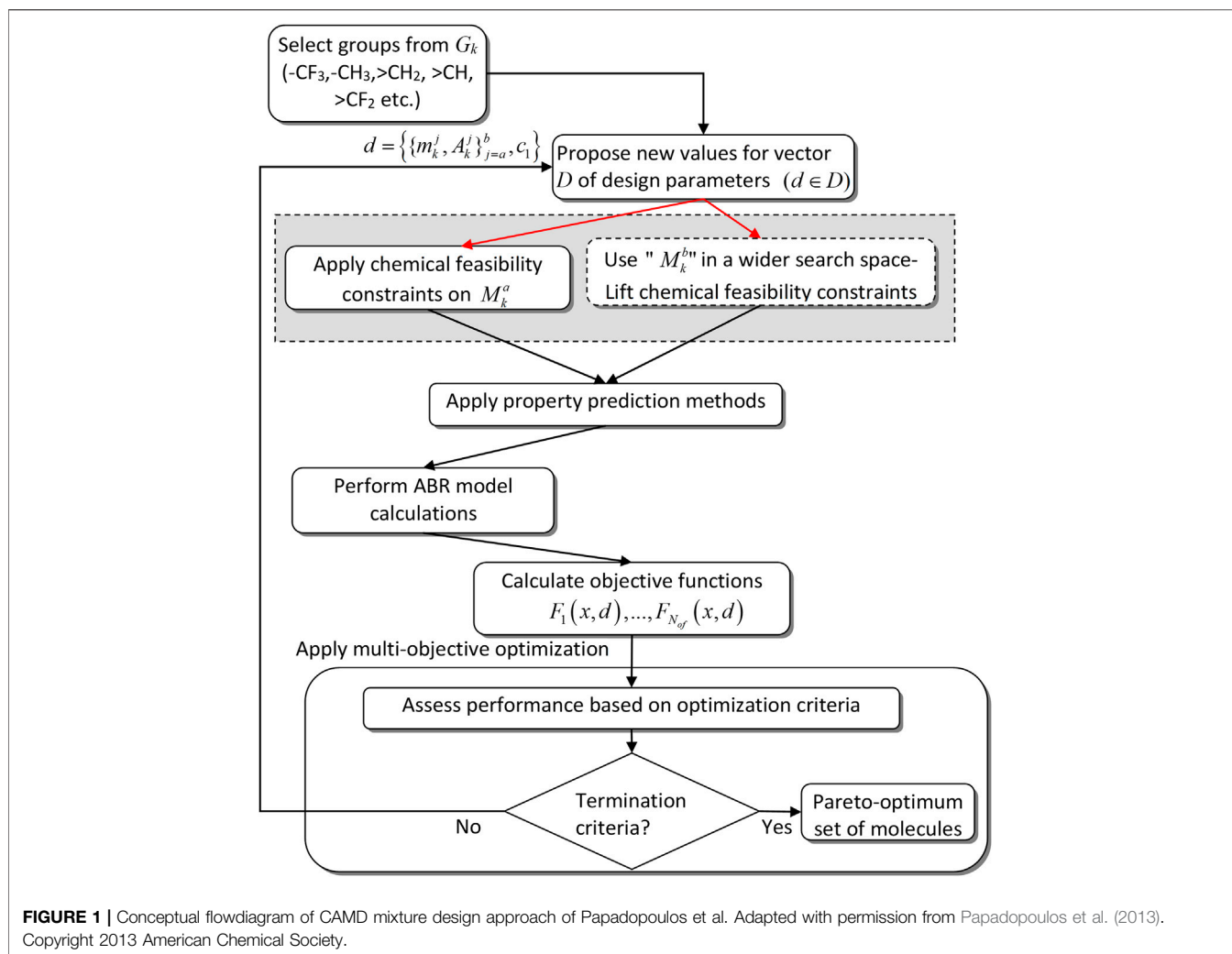
The working fluid mixture used in ABR affects significantly the cycle efficiency. Published research efforts document working fluids that include inorganics (Sun et al., 2012), ionic liquids (Khamooshi et al., 2013), and organics (Papadopoulos et al., 2019). The most widely considered inorganic options include $H_2O/LiBr$ and NH_3/H_2O, which are the only fluids that are used in commercial-level applications (Papadopoulos et al., 2019). The negligible vapor pressure of LiBr makes it a very good absorbent and simplifies the operation of the ABR as the separation of the mixture during heat addition is easy. However, salt mixtures exhibit crystallization issues if the ABR operation exceeds specific concentration limits, whereas the use of H_2O as a refrigerant prohibits generation of cooling below 0°C (Ghafoor and Munir, 2015). The latter may be overcome using NH_3 as a refrigerant, however it generally exhibits toxicity issues and requires efficient separation from water during heat addition (Papadopoulos et al., 2019). Ionic liquids represent a promising type of fluids as absorbents due to their negligible vapor pressure (Khamooshi et al., 2013). However, only very few such fluids have been investigated in the past (Khamooshi et al., 2013), while they generally exhibit high viscosity and are much more expensive than other options (Papadopoulos et al., 2019). Organics have received attention in published literature as alternatives to the two commercial options (recent review in (Papadopoulos et al., 2019)). They have the potential to overcome the disadvantages of inorganics and ionic liquids and to exhibit higher performance in terms of ABR costs, health, safety and environmental impacts. They have not been considered in commercial implementations because only very few options have been investigated as refrigerants or absorbents (Papadopoulos et al., 2019). The consideration of few organic fluid mixtures in ABR literature is due to the predominant use of trial-and-error approaches in their selection. Building on know-how that is drawn mainly from conventional refrigeration systems, the majority of available works consider few cases of refrigerants and absorbents which are investigated repeatedly. Although useful, this approach can only result in limited performance improvements.

To address these challenges, the works of Tora (Tora, 2013) and Louaer et al. (Louaer et al., 2007) are the only ones that consider systematic approaches for the identification of efficient refrigerants and/or absorbents. Tora (Tora, 2013) proposes a CAMD (computer-aided molecular design) approach (Papadopoulos et al., 2018) for the identification of working fluids, implemented through the ICAS software (ICAS, 2019). CAMD approaches enable the generation of molecular structures using functional groups as building blocks, hence they are efficient in proposing molecules that may have not been considered before for a particular application. CAMD is based on the systematic combination of functional groups to synthesize molecular structures whose properties are evaluated using group contribution models (Austin et al., 2016a; Papadopoulos et al., 2018). The molecular, mixture or process properties are used as design targets so that the employed synthesis algorithm can identify the structure(s) which meet these targets. In the work of Tora (Tora, 2013) this is done in a step-wise procedure. The refrigerants are first identified using pure component properties as performance criteria, separately from the absorbents.

Absorbents are then identified considering only their solubility in the previously identified refrigerants. Few refrigerant-absorbent mixtures are formed and then tested in ABR process simulations to identify their COP (Papadopoulos et al., 2019). This approach employs molecular and mixture properties as performance criteria for the identification of molecular options that meet specific performance limits which need to be overcome. The properties associate molecular level information with operating requirements of the ABR process. While this is useful, the lack of an ABR model in the course of CAMD prohibits the evaluation of the mixtures at the temperature and pressure conditions imposed by the interactions of the mixture components and the ABR equipment. The separate, initial evaluation of refrigerants and absorbents may prematurely exclude options which could potentially lead to high ABR performance. Furthermore, different mixtures may operate in an optimum way in terms of COP or other ABR performance indicators for different values of important design parameters. For example, the optimum number of separation stages or flowrates of absorbent and refrigerant may be different for each mixture. The work of Tora (Tora, 2013) is promising, but optimization of ABR parameters is further needed in order to enable the designed mixtures to overcome the performance of conventional working fluids such as $H_2O/LiBr$ or NH_3/H_2O.

Louaer et al. (Louaer et al., 2007) investigate and identify novel and existing refrigerants which are combined with known absorbents in single-effect absorption cooling systems. The refrigerants result as combinations of functional groups, including carbon atoms with one to four free bonds and fluorine. The authors consider combinations with up to two intermediate groups which end in either fluorine or methyl groups. Using pure component properties as criteria the authors propose 10 structures which are combined with pre-specified absorbents into 40 mixtures. The latter are evaluated in single-effect ABR simulations in terms of COP and circulation ratio. Similarly to Tora (Tora, 2013), the approach of Louaer et al. (Louaer et al., 2007) exploits group-contribution models for property predictions, which allow the generation of molecular structures (Papadopoulos et al., 2018). In this case the evaluation of the refrigerant structures is exhaustive, as all the structures that may be attained as combinations of the available functional groups are generated and evaluated. However, this is done within a narrow range of groups and chemical families (i.e., small hydrofluorocarbons), hence limiting the number of molecules that may be evaluated. The authors only design refrigerants and not absorbents as in Tora (Tora, 2013). Finally, the ABR process is not optimized.

Clearly, there is a lot of scope for the simultaneous design of the mixture components as both Tora (Tora, 2013) and Louaer et al. (Louaer et al., 2007) address the design or selection of each component at separate stages. The identification of a suitable mixture with desired behavior in the process where it is utilized (i.e., the mixture design and selection problem) is much more challenging than the design and selection of a pure compound. According to Papadopoulos et al. (Papadopoulos et al., 2018) the mixture design and selection problem requires the determination of 1) the number of components in the mixture, 2) the molecular

FIGURE 1 | Conceptual flowdiagram of CAMD mixture design approach of Papadopoulos et al. Adapted with permission from Papadopoulos et al. (2013). Copyright 2013 American Chemical Society.

structure of each component and 3) the concentration of each component in the mixture. Considering that there is practically a vast number of chemicals which could be candidates for any application, it becomes clear that the problem's combinatorial complexity is very challenging. CAMD is a technology previously implemented in various applications to address such challenges (Achenie et al., 2003). In this context, several works proposed methods for mixture design and selection. Ng et al. (Ng et al., 2015b), Papadopoulos et al. (Papadopoulos et al., 2018), Austin et al. (Austin et al., 2016a), and Zhang et al. (Zhang et al., 2018; Zhang et al., 2020) published comprehensive reviews of such approaches. Few works address the design of two mixture components through CAMD (Buxton et al., 1999; Papadopoulos et al., 2013; Austin et al., 2016b; Austin et al., 2017), with even fewer works addressing the complete mixture design problem discussed previously (Jonuzaj et al., 2016; Jonuzaj and Adjiman, 2017; Jonuzaj et al., 2018). At the same time, several important approaches that also account for process models as part of mixture design also exist (Buxton et al., 1999; Van Dyk and Nieuwoudt, 2000; Sinha et al., 2003; Papadopoulos et al., 2013; Ng et al., 2015a; Cignitti et al., 2018; Liu et al., 2019). Such

features indicate that available CAMD technologies are quite advanced compared to the promising approaches of Tora (Tora, 2013) and Louaer et al. (Louaer et al., 2007), hence considerable improvements may be expected.

In this work, we propose the use of an approach for the design of binary working fluid mixtures considering a model that performs ABR process calculations in the course of CAMD. Unlike Tora (Tora, 2013), our work enables the simultaneous evaluation of both refrigerant and absorbent structures based on ABR process performance indicators during CAMD. In this respect, it is possible to directly synthesize and obtain both refrigerants and absorbents. Unlike Louaer et al. (Louaer et al., 2007), the approach does not require exhaustive evaluation of the attainable functional group combinations. Instead, the synthesis of molecular structures from functional groups is guided by an optimization algorithm (Papadopoulos et al., 2013). This allows the evaluation of only a small fraction of the molecular structures that can be attained from the available functional groups, for the identification of a rich set of mixtures that exhibit optimum performance (Samudra and Sahinidis, 2013). Finally, for the set of the designed mixtures, we implement ABR process optimization

over a wide set of important ABR design parameters, prior to selecting the optimum working fluid mixture and ABR process characteristics. Selected mixtures are further evaluated in terms of several safety, health and environmental impact indicators.

METHODS AND MODELS

Computer-Aided Molecular and Process Design of Mixtures

In this work, we adopt and further adapt the approach of Papadopoulos et al. (Papadopoulos et al., 2013) for mixture design. The latter includes two stages for the determination of the chemical structures of both components in binary mixtures. Stage 1 is called mixture screening and the corresponding CAMD algorithm is shown in **Figure 1**. The aim of Stage 1 is to determine optimum molecular structures for the first component of the mixture. This is approached by searching for chemically feasible molecular structures only for one of the two components. The mixture behavior of the remaining component is emulated within a much wider structural design space by removing the chemical feasibility constraints. This serves to evaluate the performance of the first component within a broad range of potential concentrations and interactions with the second component, prior to resulting in an inclusive set of molecular structures and properties for the two components. The identification of multiple optimum mixture candidates is accomplished through a multi-objective formulation of the CAMD optimization problem. Multiple performance measures are treated simultaneously and a comprehensive Pareto front is obtained that reveals useful structural and property trade-offs among the mixture components. In Stage 2, called the *mixture design* problem, each one of the feasible components designed in Stage 1 are used as a fixed option in a CAMD problem that identifies a feasible structure for the second component and re-evaluates the mixture concentration.
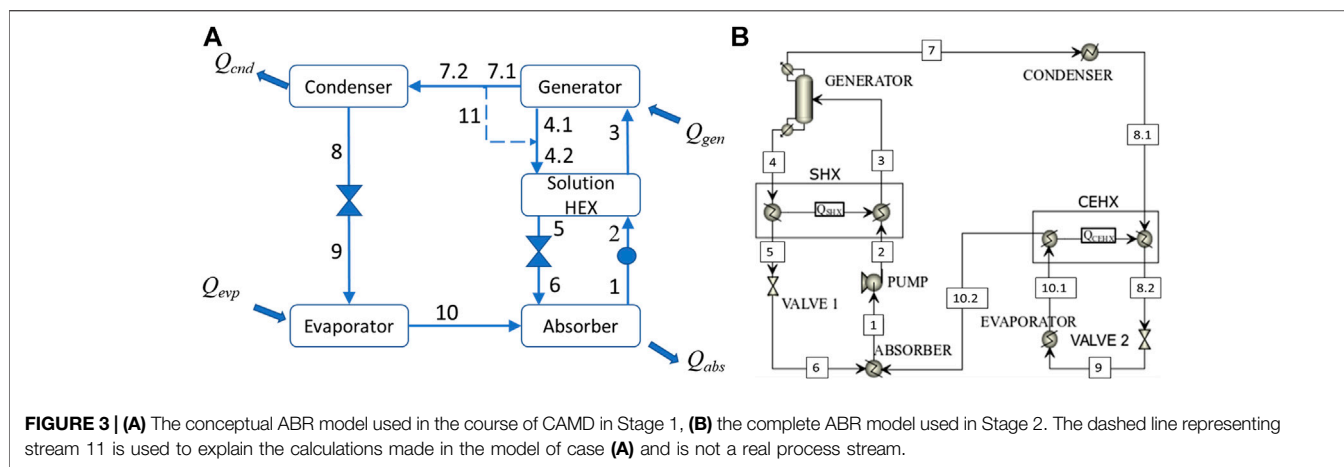
To better explain the approach used in Stage 1, assume a set of functional groups G_k which will be used as building blocks to synthesize molecular structures for both components, where k represents the number of functional groups that are selected in each iteration of the algorithm in **Figure 1**. Further assume that the first component of the mixture is M_k^a and the second component is "M_k^b." Each one is a molecular structure M_k defined as the product of vector m_k^j that contains the type of functional groups in the structure of each component j in the mixture and of the diagonal matrix A_k^j that indicates the number of functional groups in each component j. The quotation marks in "M_k^b" indicate that component b may be chemically infeasible, whereas their lack underlines the chemical feasibility of component a. Chemical infeasibility indicates that the molecular structure is not feasible in practice because it violates chemical constraints (e.g., valence etc.). However, the properties of such a structure can be calculated by the corresponding models and can still be used to perform mathematically valid ABR simulations. Vector D indicates the design parameters in the optimization problem, which include the molecular structure M_k (i.e., the type and number of
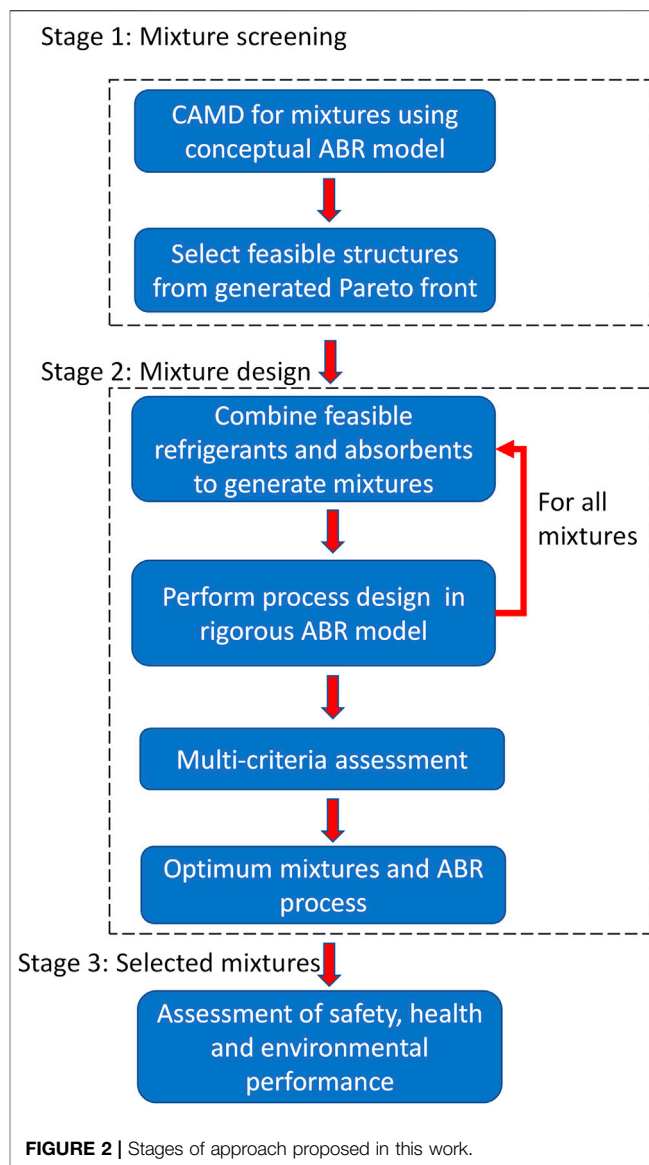
FIGURE 2 | Stages of approach proposed in this work.

functional groups comprising it) and the mixture concentration c_1, with $d \in D$ (Papadopoulos et al., 2013). The algorithm proposes molecular structures iteratively, property prediction models are applied in each iteration and the resulting data are used within an ABR process model to calculate the necessary performance indicators $F_t(x, d), t = [1, N_{of}]$, with x being the state variables of the ABR model. In the end, the Pareto optimum solution includes feasible molecular structures for component M_k^a. Those may represent novel molecules that have not been previously synthesized in practice or known, commercially available molecules.

In the current work, either of M_k^a or "M_k^b" may be the refrigerant or the absorbent. This is because we allow the algorithm to generate the two structures and to then determine the roles of each structure in the ABR process; the one with the lower boiling point (or higher vapor pressure) is

FIGURE 3 | (A) The conceptual ABR model used in the course of CAMD in Stage 1, **(B)** the complete ABR model used in Stage 2. The dashed line representing stream 11 is used to explain the calculations made in the model of case **(A)** and is not a real process stream.

TABLE 1 | Assumptions for the ABR model simulations performed in this work.

Stream	Stage 1 ABR model		Stage 2 ABR model	
	State	Composition	State	Composition
1	Saturated liquid	Mixture	Saturated liquid	Mixture
2	Subcooled liquid	Mixture	Subcooled liquid	Mixture
3	Subcooled liquid	Mixture	Subcooled liquid	Mixture
4.1	Saturated liquid	Mixture	Saturated liquid	Mixture
4.2	Saturated liquid	Mixture		
5	Subcooled liquid	Mixture	Subcooled liquid	Mixture
6	Vapor-liquid	Mixture	Vapor-liquid	Mixture
7.1	Superheated vapor	Refrigerant with absorbent (small amount)	Superheated vapor	Refrigerant with absorbent (small amount)
7.2	Superheated vapor	Pure refrigerant		
8.1	Saturated liquid	Pure refrigerant	Saturated liquid	Refrigerant with absorbent (small amount)
8.2			Subcooled liquid	Refrigerant with absorbent (small amount)
9	Vapor-liquid	Pure refrigerant	Vapor-liquid	Refrigerant with absorbent (small amount)
10.1	Saturated vapor	Pure refrigerant	Saturated vapor with small amount of liquid	Refrigerant with absorbent (small amount)
10.2			Superheated vapor	Refrigerant with absorbent (small amount)
11	Saturated liquid	Pure absorbent	—	—

considered as the refrigerant and the one with the higher boiling point (or lower vapor pressure) as the absorbent. In this respect, both refrigerants and absorbents are evaluated in mixtures in terms of their ABR process performance. The resulting $M^{a,opt}$ in the Pareto front (i.e., the feasible structures) may contain either option. In this respect, the feasible absorbents and refrigerants are directly selected in Stage 1 and introduced into Stage 2 (**Figure 2**), where they are combined exhaustively and used into ABR process simulations. The latter enable the determination of the optimum concentration for each mixture, together with the optimum structural and operating features for the ABR. The optimization is performed through exhaustive evaluation of several parameter combinations within a wide range. Such parameters include the number of separation stages in the ABR generator, the mass flowrates of the refrigerant and the absorbent and the distillate-to-feed ratio in the generator. **Figure 2** shows that Stage 2 does not necessitate the consideration of the infeasible structures, as in the original, general mixture design approach of Papadopoulos et al. (Papadopoulos et al., 2013). The differences between the

conceptual and the more rigorous process models used in each stage are discussed in the next section. A third stage is added in the proposed approach involving post-assessment of highly performing working fluids selected in Stage 2 in terms of health, safety and environmental performance.

ABR Models

This work employs two single effect ABR models of different fidelity in the two stages. A conceptual ABR model with certain simplifications in unit operations is used in Stage 1, whereas Stage 2 employs a complete, rigorous ABR model. **Figure 3A** illustrates the basic features of the conceptual ABR model used in Stage 1. **Table 1** illustrates the states and compositions of the models used in Stage 1 and Stage 2.

The rationale of the conceptual model used during CAMD in Stage 1 is to facilitate calculations, while capturing important, operating ABR trade-offs. The proposed conceptual model represents sufficiently important driving forces including:

(1) the ease of separation of the refrigerant in the generator,

(2) the cooling output of the process,
(3) the mutual solubility of the two mixture components.

With respect to point (a), it is assumed that the generator separates as much refrigerant as possible in a single step (i.e., a flash) from the mixture that enters in stream 3 and no additional rectification is considered. This is reasonable because a mixture that results in a lower purity of refrigerant in a single-step separator will potentially require a rectifier with more separation stages in order to achieve the desired, high purity specification compared to a mixture that results in a higher purity of refrigerant. In other words, it is not necessary to design the entire rectifier in order to evaluate the ease of separation of different mixtures. The lack of a rectifier is compensated by several assumptions made in the model. Stream 7.1 in the generator output contains a mixture of refrigerant and absorbent. After assessment of the separation efficiency, it is assumed that the refrigerant is entirely removed from the absorbent in stream 7.2 and that the removed absorbent quantity is returned through stream 11 to stream 4.2. It is further assumed that some condensation occurs in order to turn the state of stream 11 into saturated liquid from superheated vapor. This is done in order to mix streams 11 and 4.1 at the same state and to facilitate calculations. In this respect, the full refrigeration potential of the cycle can be evaluated as the absorbent does not remain in the stream that goes into the condenser. This is reasonable because a rectifier with an appropriate number of stages would eventually be able to separate (almost) all the absorbent from the refrigerant and to eventually achieve a high refrigerant purity.

The proposed simplification addresses the previously noted point (b), while another simplification in the refrigeration circuit pertains to the lack of a condenser-evaporator heat exchanger (CEHX), which is used in a complete ABR model as shown in **Figure 3B**. The CEHX is used to reduce the temperature of the saturated liquid out of the condenser and facilitates the generation of a sub-cooled liquid. This eventually allows a lower amount of vapor to be generated after the expansion and increases the efficiency of the evaporator. This unit operation is therefore not critical in the context of CAMD which compares different mixtures in terms of COP. The mixtures that result from CAMD may exhibit a slightly lower COP than the one that is attained through the model of **Figure 3B**. However, this simplification in the ABR model used during CAMD is sufficient in order to identify and avoid poorly performing mixtures. With respect to point (c), in the absorber we assume that all the refrigerant vapor is efficiently absorbed into the incoming liquid and we assess the solubility of the two components through their solubility parameter values. This is the only point in the model of **Figure 2A** where we use molecular properties instead of process-level calculations. Again, this simplification serves to facilitate calculations and is sufficient to avoid the selection of refrigerants and absorbents that exhibit poor miscibility, hence they are likely to prohibit the design of an efficient absorber.

As shown in **Table 1**, the model in Stage 2 does not employ such simplifications. The generator is modelled through a distillation column. By investigating different parameters such as the number of stages and the distillate-to-feed ratio we are able to assess the requirements in order to achieve a separation that will result in a refrigerant outlet stream of high purity. The absorber includes all necessary calculations and fully accounts for the miscibility of the two components within the processing conditions.

CAMD Optimization Problem Formulation

In Stage 1 of the proposed approach, the mixture screening problem is formulated as follows:

$$\max_{d \in D} COP, y_{gen,out}^{ref}, \tag{1}$$

$$\min_{d \in D} y_{throt,out}^{ref}, Q_{cnd}, \tag{2}$$

$$s.t.$$

$$T_{throt,in} - T_{pump,out} > \Delta T, \tag{3}$$

$$T_{hex,in} - T_{hex,out} > \Delta T, \tag{4}$$

$$P_{high} > 1, \tag{5}$$

$$\left| \delta_s^{ref} - \delta_s^{abs} \right| < \varepsilon_1, \tag{6}$$

$$T_b^{abs} - T_b^{ref} > \varepsilon_2, \tag{7}$$

$$\max\left(T_m^{ref}, T_m^{abs} \right) < T_{evp,out} - \varepsilon_3, \tag{8}$$

$$\sum_{i \in \{ref,abs\}} x^i = 1, \tag{9}$$

where $d = \{\{m_k^j, A_k^j\}_{j=a}^b, z^{ref}\}$ and z^{ref} represents the mole fraction of the refrigerant. The employed objective functions include the maximization of COP and of the refrigerant purity $y_{gen,out}^{ref}$ at the generator outlet stream 7.1, while minimizing the vapor fraction of the refrigerant $y_{throt,out}^{ref}$ after throttling at the refrigeration circuit, i.e., stream 9, and the heat quantity removed at the condenser Q_{cnd}. The COP and $y_{gen,out}^{ref}$ are complementary objectives, as the maximization of $y_{gen,out}^{ref}$ will result in an increase of the COP. On the other hand, using either of the objectives without the other would not guarantee that they could both be maximized. Regarding $y_{throt,out}^{ref}$, it is clearly desired to have saturated liquid entering the evaporator, hence any vapor should be avoided in stream 9. In this respect, $y_{throt,out}^{ref}$ supports the maximization of COP and is therefore complementary to it. Finally, Q_{cnd} is associated with the size of the condenser and with the auxiliary cooling requirements, hence it is not directly linked with the other objectives. Constraints **Eqs. 3,4** aim to avert the violation of a minimum temperature difference ΔT which is necessary to allow heat transfer. $T_{throt,in}$ refers to stream 5, $T_{pump,out}$ refers to stream 2, $T_{hex,in}$ refers to stream 4.2 and $T_{hex,out}$ refers to stream 3. Constraint **Eq. 5** indicates the desire to have at least one of the two pressures higher than 1 bar and to avoid having the entire system operating in vacuum. Constraint **Eq. 6** indicates the desire for good solubility between the two components, to enable efficient absorption. It is expressed through the difference of the Hansen solubility parameter δ_s

(Hansen, 2004) of the two components. Constraint **Eq. 7** imposes a minimum boiling point difference in order to facilitate good separation of the two components, whereas constraint **Eq. 8** indicates that the component with the maximum melting point T_m should exhibit a melting point temperature at least several degrees ε_3 lower than the evaporator temperature $T_{evp,out}$ in order to avoid solidification. The latter temperature refers to stream 10. These are indicative objective functions and constraints that are proven to result in relevant refrigerants and absorbents, as shown in the subsequent sections. Different or additional ones may also be used.

The simultaneous evaluation of the objectives in **Eqs. 1,2** is performed based on the satisfaction of a specific condition. Assume that each one of the terms in **Eqs. 1** is part of vector $F = F_t(x, d), t = [1, N_{of}]$ of objective functions, i.e., $F_1 = COP$, $F_2 = y^{ref}_{gen,out}$, $F_3 = y^{ref}_{throt,out}$, $F_4 = Q_{cnd}$. Based on Papadopoulos et al. (Papadopoulos et al., 2013), an instance of the design vector $d \in D$ (i.e., mixture components and concentration) is called a Pareto optimum or non-dominated solution *iff* there exists no other $d^* \in D$ satisfying the following condition:

$$F(d^*) \leq F(d) \wedge \exists t \in \left\{1, ..N_{of}\right\} : F_t(d^*) < F_t(d), \quad (10)$$

The mixtures that are generated during CAMD are compared in terms of their objective function values, with the ones satisfying condition **Eq. 10** entering the Pareto front.

From Stage 1 we obtain a vector of chemically feasible $M^{a,opt}$ structures which include both refrigerants and absorbents. In stage 2, we combine these structures of Stage 1 into mixtures. The resulting mixtures are introduced and evaluated in ABR process design using the model illustrated in **Figure 3B**. The mixture and ABR process design problem is formulated as follows:

$$\max_{M^{a,opt}, N_p} COP, n_{ex}, ds/f, \quad (11)$$

$$\min_{M^{a,opt}, N_p} P_{high}, \dot{m}^{ref}, \dot{m}^{abs}, n^{stage}, \quad (12)$$

$$s.t.$$

$$y^{ref}_{gen,out} \geq y^{ref,lim}_{gen,out}, \quad (13)$$

$$\sum_{i \in \{ref,abs\}} y^i_{pump,in} = 0, \quad (14)$$

$$\sum_{i \in \{ref,abs\}} y^i_{throt,out} \leq y^{lim}_{throt,out}, \quad (15)$$

$$ds/f^L \leq ds/f \leq (ds/f)^U, \quad (16)$$

$$\dot{m}^L_{ref} \leq \dot{m}_{ref} \leq \dot{m}^U_{ref}, \quad (17)$$

$$\dot{m}^L_{abs} \leq \dot{m}_{abs} \leq \dot{m}^L_{abs}, \quad (18)$$

$$n^{stage,L} \leq n^{stage} \leq n^{stage,U}, \quad (19)$$

where $N_p = \{ds/f, n^{stage}, \dot{m}^{ref}, \dot{m}^{abs}\}$ is a set including the design parameters of the ABR process. In this case we are seeking mixtures with maximum COP, exergy efficiency n_{ex} and distillate-to-feed ratio, expressed as ds/f. The latter represents the desire to enable high recovery at the generator outlet stream that is led to the condenser. Since the refrigerant is the compound

that should be recovered, this ratio is complemented by constraint **Eq. 13** which imposes a lower limit on the purity of the refrigerant in the same stream. Note that f refers to the flowrate of stream 3, whereas ds and $y^{ref}_{gen,out}$ refer to the flowrate and vapor fraction of stream 7. At the same time, mixtures should exhibit minimum P_{high} to avoid the need for expensive equipment that can withstand high pressures, and minimum absorbent and refrigerant flowrates $\dot{m}^{ref}$ and $\dot{m}^{abs}$, referring to stream 1. We also require mixtures that are separated in the smallest number of stages n^{stage} possible, as the latter is associated with the size and economics of the rectifier. By varying the parameters in N_p we identify the optimum design and operating characteristics of the ABR for each, specific mixture. Most of these objective functions affect the COP and at the same time are necessary because they are also associated with other design issues, such as sizes of equipment. The number of stages is clearly associated with the distillate-to-feed ratio (i.e., the reduction of the stages in the rectifier is likely to result in lower ratio), hence they represent opposite trends in the multi-criteria formulation. The same holds for the mass flowrates and the COP or the exergetic efficiency; lower flowrates may lead to reduction of these two indicators, hence there is clearly an opposite trend here too. In thermodynamic cycles that use mixtures as working fluids the thermodynamic efficiency (expressed here through COP) and the exergetic efficiency are generally known to follow opposite trends (Papadopoulos et al., 2013). **Eq. 14** indicates that vapor is not allowed to enter the pump in stream 9. **Eq. 15** indicates that the vapor fraction in stream 7 should be below an upper limit as the introduction of vapor in the evaporator reduces the generated cooling, with detrimental effects on COP. Note that **Eqs. 3,4** still hold in this model too, however they are evaluated implicitly by the employed software hence they are not included in the formulation.

Equations. 11–19 will generate a sufficiently inclusive Pareto front D'_{opt}, comprising the desired mixtures and the corresponding ABR specifications in N_p. However, our aim in this work is to generate more comprehensive insights regarding the trade-offs among different performance indicators. We therefore transform relations **Eqs. 11,12** into an aggregate index to then generate Pareto fronts between this index and each indicator. This further allows us to determine how the overall performance (i.e., in all indicators considered simultaneously) of each working fluid is affected by changes in each indicator separately. Specifically for the set of performance indicators $Pr = \{COP, n_{ex}, ds/f, P_{high}, \dot{m}_{ref}, \dot{m}_{abs}, n^{stage}\}$ and for the mixtures in D'_{opt} we propose an aggregate index J which merges the properties under a unified criterion that satisfies the selection goals described in **Eqs 11** (i.e. the simultaneous minimization and maximization of the corresponding properties), as follows:

$$\min_{i \in D'_{opt}} J_i = \sum_{q \in P_r} a_{i,q} \cdot x^*_{i,q}, \quad (20)$$

where $x^*_{i,q}$ represents the considered scaled indicator in P_r for each working fluid mixture i, and $a_{i,q}$ represents a unity coefficient that is positive for properties that need to be minimized and negative for those to be maximized. Based on **Eq. 20**, the selection of

working fluid mixtures with increased performance translates to the minimization of index J_i. The multi-criteria selection problem that is solved includes the identification of the Pareto indicators by generation of a Pareto front per indicator $q \in \mathrm{Pr}$, considering the index J for all $i \in D'_{opt}$ against each one of the indicators represented through their values $x_{i,q}$. The problem is formulated as follows:

$$\min_{i \in D'_{opt}} J_i, \qquad (21)$$

$$\min_{q \in \mathrm{Pr}} or \max_{q \in \mathrm{Pr}} q. \qquad (22)$$

subject to **Eqs. 13–19**. Solving this problem results in seven Pareto fronts of J against the corresponding properties in Pr. Note that **Eq. 10** is applied for both formulations **Eqs. 11–12** and **Eqs. 21–22** in order to derive the Pareto optimal mixtures. Additional details can be found in Zarogiannis et al. (Zarogiannis et al., 2016).

Assessment of Safety, Health and Environmental Impact Properties

The working fluids that are selected as highly performing options using the previously described approach may then be evaluated in terms of safety, health and environmental impacts during their use in the ABR process. The evaluation pertains to the refrigerant and the absorbent comprising each mixture because mixture models considering non-idealities are only available for few properties (e.g., flammability (Papadopoulos et al., 2013)), while the corresponding calculations may be tedious.

(1) The properties considered to evaluate the safety of the components include the flash point F_p as a measure of flammability (Hukkerikar et al., 2012a) and the explosiveness S, expressed as the difference between the upper and lower flammability limits of the compound (Ten et al., 2016). Chemicals of low flammability are those that exhibit high F_p, whereas minimum S is desired.

(2) The properties considered to evaluate the health impacts of the components include the oral rat acute toxicity LD_{50} and the permissible exposure limit PEL. It is desired to use chemicals that exhibit minimum $-\mathrm{Log}(LD_{50})$ and $-\mathrm{Log}(PEL)$ (Ten et al., 2016).

(3) Regarding environmental impacts, it is desired to use chemicals that exhibit high biodegradation probability P_{BIODEG} (Wennberg and Petersen, 2017), short half-life HL in the atmosphere (EPI suite, 2019), low soil-sorption coefficient K_{OC} (ChemSafetyPro, 2019b), bioconcentration factor BCF (ChemSafetyPro, 2019a), vapor pressure P_{vp}, and water solubility W_s (Ten et al., 2016). P_{BIODEG} pertains to rapid aerobic degradation of the chemical, HL indicates the potential for atmospheric oxidation, K_{OC} indicates the adsorption of the chemical into the soil and BCF indicates tendency for accumulation in organisms. The final two properties provide an indirect indication of environmental impacts, with P_{vp} showing losses in the atmosphere and W_s indicating the ease of separation of the chemical from water.

TABLE 2 | Range within which the parameters are varied.

Parameter	Lower limit	Upper limit	Step s
ds/f	0.05	0.6	0.05
n^{stage}	4	12	1

IMPLEMENTATION

Stage 1 includes the following set of functional groups as options in CAMD: CH_3, CH_2, CH, C, OH, $CH_3(C=O)$, $CH_2(C=O)$, $CH(C=O)$, $H(C=O)$, CH_3COO, CH_2COO, $HCOO$, CH_3O, CH_2O, CHO, CH_2CN, $COOH$, CF_3, CF_2. These groups are selected based 1) oν a prior assessment of the structural characteristics of absorbents reported in published literature (Papadopoulos et al., 2019), and 2) on the availability of models and group contribution data for the prediction of the properties which are necessary in the corresponding simulations. The maximum size of the molecule is 16, whereas up to eight different groups are allowed to appear in each molecule. In this respect the maximum, attainable structural space for each one of the mixture components is $2.2 * 10^6$ structures, based on (Samudra and Sahinidis, 2013). Considering that the mixture concentration is an additional, continuous parameter, the combinatorial problem is very challenging, yet manageable by CAMD implementations (Samudra and Sahinidis, 2013).

In stage 1, thermodynamic calculations are performed using the Soave-Redlich-Kwong (SRK) EoS as implemented in (Assael et al., 1996) with UNIFAC as described in (Reid et al., 1987) and with interaction parameters from the same source. All group contribution models are based on Hukkerikar et al. (Hukkerikar et al., 2012b), except for ideal gas molar heat capacities which are based on Buxton et al. (Buxton et al., 1999). Condenser and absorber temperatures T_{cnd}^{out} and T_{abs}^{out} are considered 40°C, whereas the evaporator temperature T_{evp}^{out} is considered 0°C. The heat source input is $Q_{gen} = 269.7$ kW. The ε_1 value in inequality **Eq. 6** is set to 7 $(\mathrm{MPa})^{0.5}$ based on a rule of thumb stating that below this value a solute is miscible in a solvent, whereas it becomes immiscible at higher values (Papadopoulos and Linke, 2006). Parameter ε_2 in inequality **Eq. 7** is set to 10°C to impose a minimum boiling point temperature difference and to ensure that there is driving force for separation. Parameter ε_3 in **Eq. 8** is also set to 10°C to ensure that the melting point temperature is sufficiently lower than the minimum cycle temperature. The efficiency of the solution heat exchanger is set to the relaxed value of 0.72 in order to avoid excluding mixtures that may not be able to allow heat exchange, if this value is higher. Parameter ΔT in **Eqs. 3** is set to 10.

In Stage 2, the model is developed using the ASPEN Plus software (AspenTech, 2019). The limits in constraints **Eqs. 13–15** include $y_{gen,out}^{ref,lim} = 0.995$ and $y_{throt,out}^{lim} = 0.11$. All limit values are set based on NH_3/H_2O which is our reference mixture and apply to all the organic mixtures investigated in this work. For $y_{gen,out}^{ref,lim}$, the value is obtained from literature sources (Adewusi and Zubair, 2004; Herold et al., 2006), while for
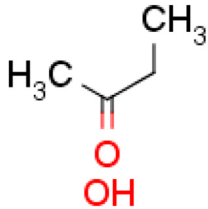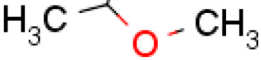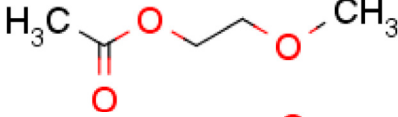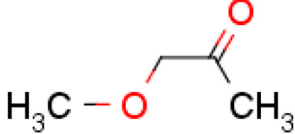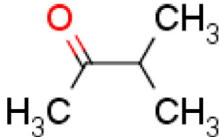
TABLE 3 | Mixtures designed in this work. An abbreviation is used in brackets, after the IUPAC names for each absorbent. Abbreviations with the letter D indicate a mixture formed by one of the refrigerants with each absorbent. For example, D1 is a mixture of Acetaldehyde/MMM.

A/A	Absorbent		Refrigerant	
			Acetaldehyde	**Butane**
A1	Methoxy(1-methoxyethoxy)methane (MMM) COCOC(C)OC CAS: -		D_1	D_{18}
A2	1-Mtehoxy-2-methylpropane (MMP) COCC(C)C CAS: 625-44-5		D_2	D_{19}
A3	1-Methoxybutan-2-one (1MOBON) CCC(=O)COC CAS: 50,741-70-3		D_3	D_{20}
A4	2-Methoxypropane (MPROP) COC(C)C CAS: 598-53-8		D_4	D_{21}
A5	Propan-2-one (PPON) CC(C)=O CAS: 67-64-1		D_5	D_{22}
A6	Ethanol (ETHOL) CCOCAS: 64-17-5		D_6	D_{23}
A7	Propan-2-yl acetate (PAC) CC(C)OC(C)=O CAS: 108-21-4		D_7	D_{24}
A8	3-Methoxybutan-2-one (3MOBON) COC(C)C(C)=O CAS: 7,742-05-1		D_8	D_{25}
A9	Methyl acetate (MAC) COC(C)=O CAS: 79-20-9		D_9	D_{26}
A10	Ethyl propanoate (EPROP) CCOC(=O)C CCAS: 105-37-3		D_{10}	D_{27}
A11	Methanediol (MDOL) OCO CAS: 463-57-0		D_{11}	D_{38}

(Continued on following page)

TABLE 3 | (*Continued*) Mixtures designed in this work. An abbreviation is used in brackets, after the IUPAC names for each absorbent. Abbreviations with the letter D indicate a mixture formed by one of the refrigerants with each absorbent. For example, D1 is a mixture of Acetaldehyde/MMM.

A/A	Absorbent	Refrigerant	
		Acetaldehyde	Butane
A12	Butan-2-one (BUTN) CCC(C)=O CAS: 78-93-3	D_{12}	D_{29}
A13	1-Methoxyethan-1-ol (MEL) COC(C)O CAS: 563-64-4	D_{13}	D_{30}
A14	Propan-1-ol (PPOL) CCCO CAS: 71-23-8	D_{14}	D_{31}
A15	2-Methoxyethyl acetate (MOEAC) COCCOC(C)=O CAS: 110-49-6	D_{15}	D_{32}
A16	1-Methoxy-propan-2-one (MOPON) COCC(C)=O CAS: 5,878-19-3	D_{16}	D_{33}
A17	3-Methylbutane-2-one (MBON) CC(C)C(C)=O CAS: 63-80-4	D_{17}	D_{34}

$y_{throt,out}^{lim}$ the value is set after simulation using input data obtained from (Adewusi and Zubair, 2004; Herold et al., 2006) for NH_3/H_2O. Here, the *SHX* effectiveness is set to 1 and the *CHX* effectiveness to 0.95. The thermodynamic package used in ASPEN Plus for vapor and liquid phase non-idealities employs the Redlich-Kwong (RK) equation of state (EoS) and UNIFAC, as they are the closest models available to the ones used in the simulations performed in Stage 1. **Table 2** illustrates the upper and lower values, as well as the step size used for the ABR design parameters ds/f and n^{stage} in the exhaustive evaluation of all mixtures introduced into the ABR model. The limits for parameters $\dot{m}_{ref}$ and $\dot{m}_{abs}$ are discussed in Papadopoulos et al. (Papadopoulos et al., 2020a), as part of a patent application. In Stage 3 of the proposed approach calculations are performed based on (Hukkerikar et al., 2012a) for F_p, LD_{50}, and *PEL*, on (Ten et al., 2016) for *S*, and on (EPI suite, 2019) for P_{BIODEG}, *HL*, K_{OC}, *BCF*, P_{vp}, and W_s, unless numbers are taken from other sources as indicated in the ESI (electronic supplementary information), where all data are presented.

A detailed analysis regarding the validation of the conceptual model of **Figure 3A** is presented in the ESI. The model was validated for Butane-Ethanol using results from the ASPEN Plus model of **Figure 3B**. The deviations between the two models in *COP*, Q_{evp} and Q_{cnd} are 13, 13 and 15%, respectively. These correspond to 0.04 COP units, and to approximately 5 kW in evaporator and condenser duties which are very small. The deviation in the total mass flowrate $\dot{m}_{tot}$ is 1%, whereas no deviation is observed in the vapor fraction of the refrigerant at the generator outlet $y_{out}^{ref,G}$. Considering the assumptions and simplifications included in the calculations of the conceptual model (e.g., use of group contribution methods, simplified modeling of the absorber etc.), the results are very satisfactory. The complete model of **Figure 3B** has been previously validated by the co-authors in Gkouletsos et al. (Gkouletsos et al., 2019) and in Papadopoulos et al. (Papadopoulos et al., 2020b), using results from literature (Adewusi and Zubair, 2004). The average absolute error in temperatures of all the cycle streams is 2.1°C, whereas the average relative error in the condenser, absorber and evaporator heat duties and in the COP is 2.9%. These results indicate very reliable predictions.

RESULTS AND DISCUSSION

Performance of Designed Mixtures

The designed refrigerants and absorbents are shown in **Table 3**. A first observation is that the two refrigerants designed are
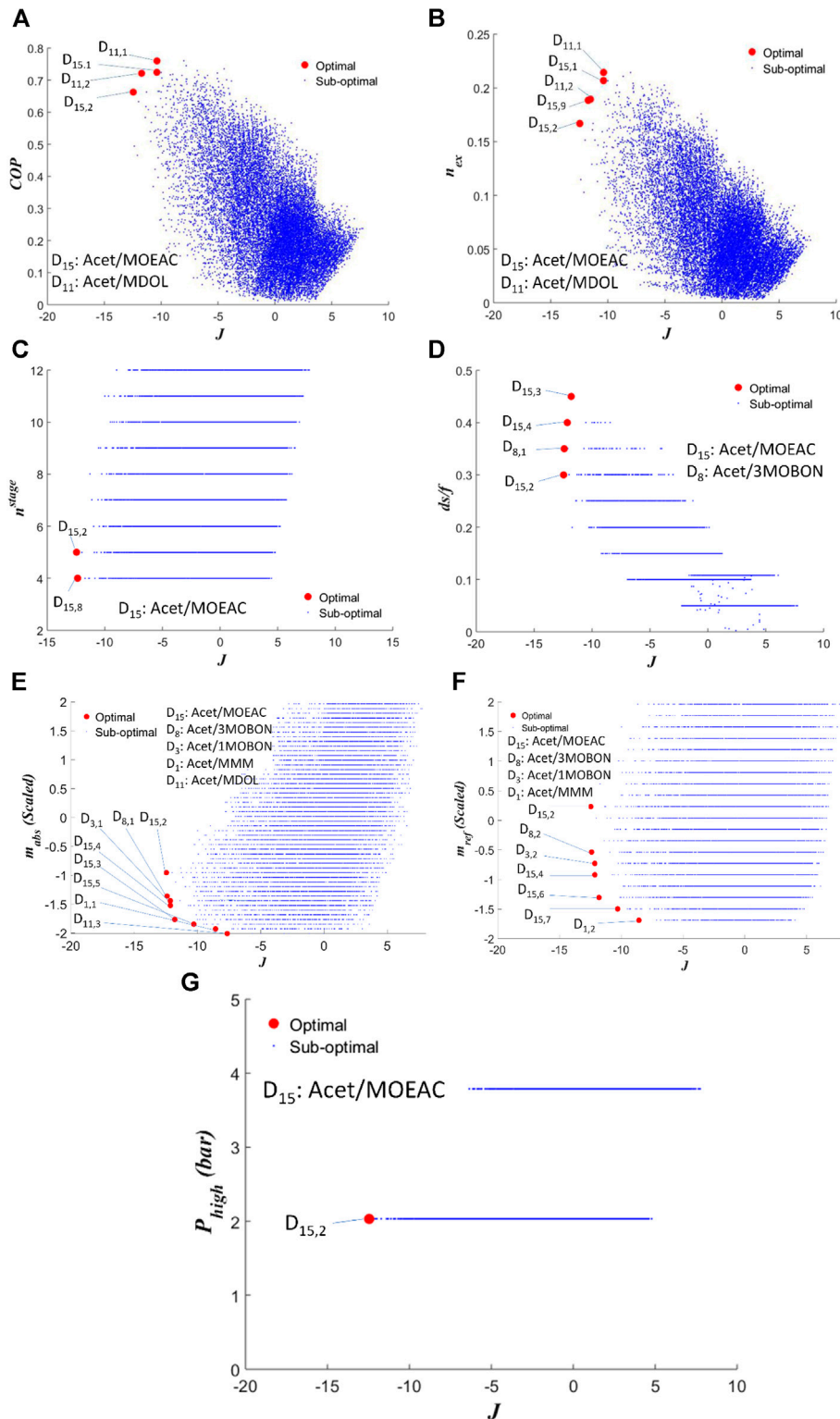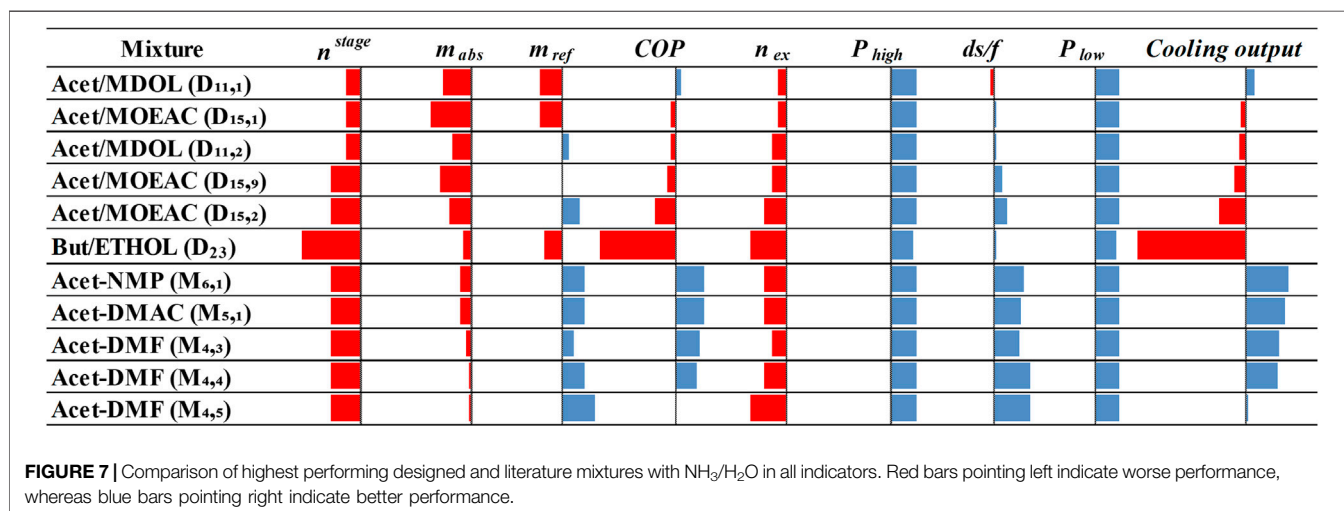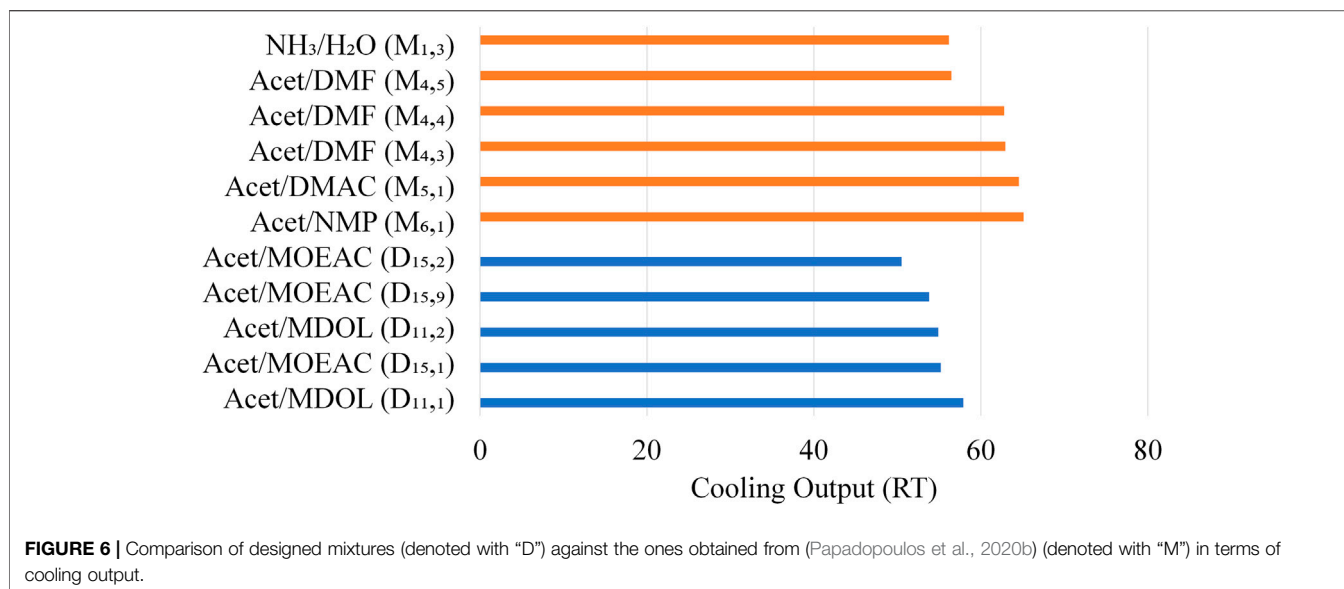
FIGURE 4 | Pareto fronts of **(A)** COP, **(B)** n_{Ex}, **(C)** n^{stage}, **(D)** ds/f, **(E)** m_{abs}, **(F)** m_{ref}, **(G)** P_{high}, vs. index J. Mixtures that appear multiple times in the same diagrams are different in one or more ABR operating parameters. This is indicated by using a second index, next to the mixture ID (e.g., $D_{15,1}$ is different to $D_{15,2}$). Such data are given only in **Supplementary Table S3** of the ESI to maintain the clarity of the figures.
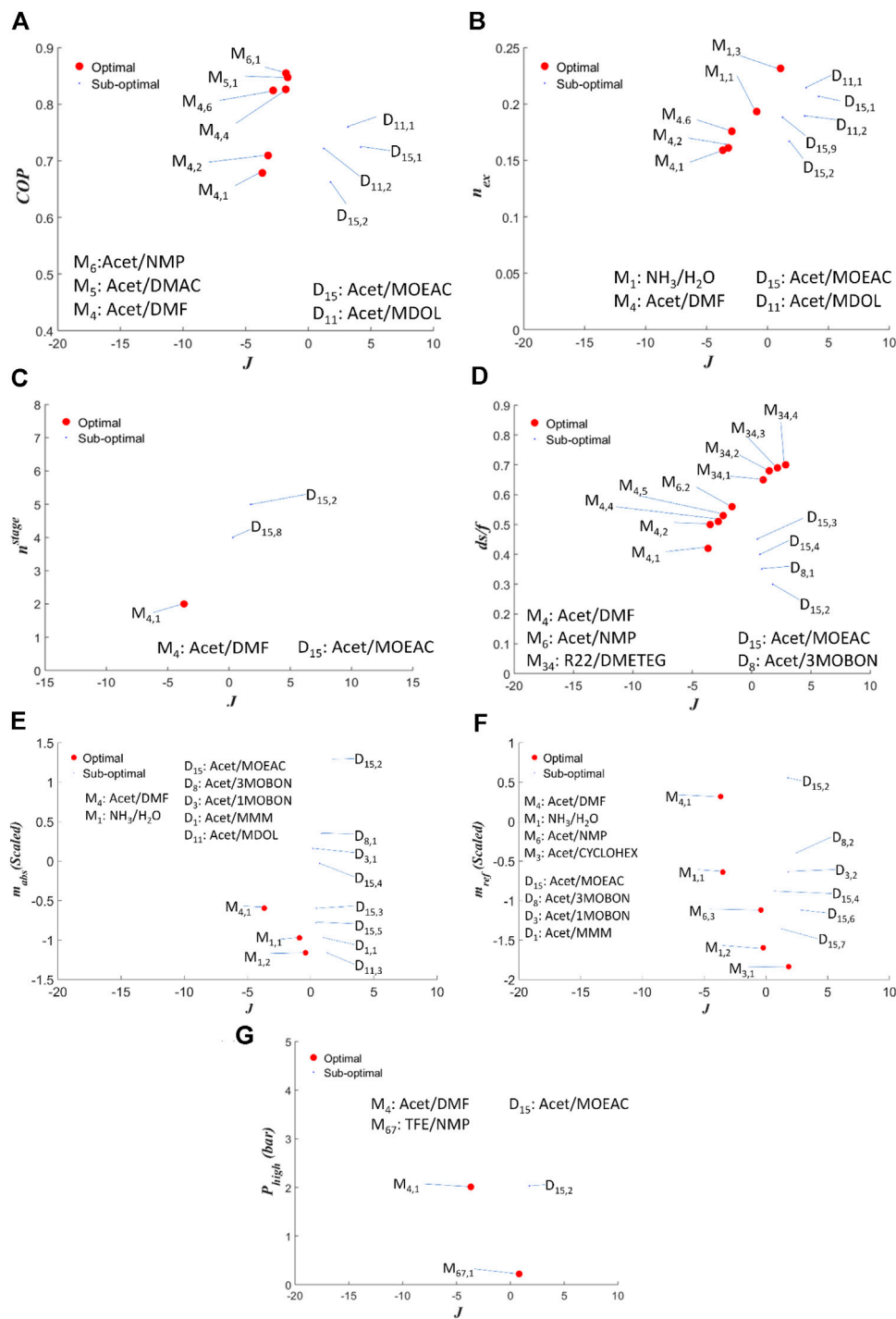
FIGURE 5 | Pareto fronts of **(A)** COP, **(B)** n_{Ex}, **(C)** n^{stage}, **(D)** ds/f, **(E)** m_{abs}, **(F)** m_{ref}, **(G)** P_{high}, vs. index J, comparing the performance of the designed mixtures ("D") with the best ones obtained from (Papadopoulos et al., 2020b) ("M").

Acetaldehyde and Butane. These were also proposed by Tora (Tora, 2013), who eventually selected a mixture with Butane. In Papadopoulos et al. (Papadopoulos et al., 2020b) we found that Acetaldehyde is the optimum refrigerant both in terms of process operation and economic performance, among several other

options identified heuristically. These are clear indications that the employed CAMD approach was able to identify two refrigerants that exhibit very high performance in ABR processes. On the other hand, Propane, Dimethyl-ether and Isobutane, previously also proposed by Tora (Tora, 2013) with

FIGURE 6 | Comparison of designed mixtures (denoted with "D") against the ones obtained from (Papadopoulos et al., 2020b) (denoted with "M") in terms of cooling output.

FIGURE 7 | Comparison of highest performing designed and literature mixtures with NH₃/H₂O in all indicators. Red bars pointing left indicate worse performance, whereas blue bars pointing right indicate better performance.

inferior performance to Acetaldehyde and Butane, were not proposed by the CAMD approach of our work. Finally, fluorinated refrigerants do not appear in the designed options which is an indication that they do not perform well, despite the attention that they received in published literature (Papadopoulos et al., 2019). In this case, we only considered groups CF_3 and CF_2 as options, hence omitting several other potential fluorocarbon chains that were considered by Louaer et al. (Louaer et al., 2007). The two groups were used because they were the only ones for which group contribution models were available for the calculation of all the properties necessary for the performed simulations. It is worth noting that various fluorinated refrigerants tested in Papadopoulos et al. (Papadopoulos et al., 2020b) exhibited inferior performance compared to Acetaldehyde, hence the consideration in CAMD of other fluorinated structures, if sufficient data were available, would almost certainly not result in highly performing solutions.

In terms of absorbents, it appears that there is a larger variety than refrigerants. The designed absorbents of **Table 3** include ethanol, acetone and 2-Methoxypropane, also identified as good candidates by Tora (Tora, 2013), who eventually chose ethanol in a mixture with Butane. This is a second clear indication that the proposed CAMD approach is able to identify ABR working fluid mixtures that exhibit high performance. Despite the identification of common refrigerants or absorbents with Tora (Tora, 2013), the mixture proposed here performs considerably better than Ethanol-Butane, as indicated below and in *Comparison of Designed Mixtures With Mixtures From Literature.* It is further worth noting that the absorbents proposed in this work include mainly ether and ketone groups, with fewer cases of carboxylic and hydroxylic groups. As shown in the review of Papadopoulos et al. (Papadopoulos et al., 2019), almost all absorbents investigated in published literature include such groups.

Component	Safety		Health		Environment					
	F_p	S	$-Log(LD_{50})$	$-Log(PEL)$	$Log(P_{vp})$	$Log(W_s)$	P_{BIODEG}	$Log(HL)$	$Log(K_{oc})$	$Log(BCF)$
BUTANE										
ACETALDEHYDE										
DMF										
DMAC										
NMP										
ETHANOL										
MDOL										
MOEAC										

FIGURE 8 | Comparison of selected working fluids with NH$_3$ in terms of safety, health and environmental impact properties. Red bars pointing left indicate worse performance, whereas blue bars pointing right indicate better performance.

The above 34 mixtures are introduced into the rigorous ABR process model used in stage 2, in order to calculate the indicators and constraints of **Eqs. 11–19**. For every mixture, the ABR design parameters of **Table 2** are varied exhaustively within the corresponding upper and lower limits (mass flowrates are also included, but mentioned explicitly in (Papadopoulos et al., 2020a)). This variation results in 108,000 ABR model simulations for each one of the mixtures.

Figures 4A–G illustrate the mixtures that exhibit an overall high performance based on the multicriteria assessment approach. To maintain clarity, we only show part of the sub-optimal points. Index J enables the generation of clear insights regarding the performance of the mixtures. For example, in **Figure 4A** it appears that D$_{15,2}$ exhibits the lowest COP among all the Pareto-optimum mixtures, but also the lowest J value. This means that D$_{15,1}$ exhibits considerably better performance in all indicators other than COP, hence it may not be a very competitive option. Mixture D$_{15}$, Acet-MOEAC appears 19 times in the Pareto fronts at various absorbent/refrigerant concentrations, D$_{11}$, Acet-MDOL appears 5 times, D$_3$, Acet-3MOBON appears 3 times, D$_8$, Acet-1MOBON and D$_1$, Acet-MMM appear 1 time. The first observation is that Butane-based or Acetone-, Ethanol- and 2-Methoxypropane-based mixtures are part of the sub-optimal solutions, not of the Pareto fronts. This indicates that the proposed approach generates mixtures of improved ABR performance compared to Tora (Tora, 2013). In fact, mixture Butane-Ethanol (D$_{23}$) exhibited a maximum COP of 0.44, requiring 7 separation stages at the generator, whereas the selected mixtures exhibit COP above 0.65 with less than 5 separation stages in the generator, to name but a few differences. Hence it is reasonable that D$_{23}$ is not part of the Pareto fronts. Mixture D$_{15}$ is one carbon atom shorter than 2-Ethoxyethyl acetate, which was previously considered in (Ando and Takeshita, 1984; Takeshita et al., 1984) with R22 as the refrigerant. Mixture D$_{11}$ includes the shortest glycol chain possible, exhibiting remarkably higher COP and n_{ex} compared to other candidates. A longer glycol, namely 1,4-Butanediol was previously proposed as an absorbent in (Tyagi, 1983). Mixtures D$_3$, D$_8$, and D$_1$ mainly show up in Pareto fronts because they enable lower refrigerant flowrates. D$_{15}$ and D$_{11}$ are also available in the Pareto fronts at low absorber and refrigerant concentrations, but in such cases

their COP values are very low. All numerical details are presented in **Supplementary Table S3** of the ESI.

Comparison of Designed Mixtures With Mixtures From Literature

Figure 5 presents a multi-criteria analysis of the mixtures that appear in the Pareto fronts of **Figure 4**, with mixtures selected arbitrarily from literature and investigated in Papadopoulos et al. (Papadopoulos et al., 2020b). The latter include NH$_3$/H$_2$O (M$_1$), Acetaldehyde/Cyclohexanone (M$_3$), Acetaldehyde/Dimethylformamide (DMF-M$_4$), Acetaldehyde/Dimethylacetamide (DMAC-M$_5$), Acetaldehyde/Methylpyrolidone (NMP-M$_6$), R22- Tetraethylene glycol dimethyl ether (DMETEG-M$_{34}$) and Trifuoro-ethanol (TFE)/NMP (M$_{67}$). The ID numbers denoted with "M" for these mixtures are the same as the ones used in Papadopoulos et al. (Papadopoulos et al., 2020b) for consistency. Note that the J values reported in **Figure 5** are not comparable with those of **Figure 4** because the scaling is now applied only in the mixtures reported in **Figure 5**. The first observation is that the designed mixtures do not overcome the performance of the mixtures selected in (Papadopoulos et al., 2020b). D$_{11}$ and D$_{15}$ are competitive options in terms of COP, n_{ex} and flowrates, as shown in the corresponding figures, but they don't exhibit high performance in all indicators simultaneously, as reflected in their higher J values. It is further worth noting that the absorbents contained in the mixtures of (Papadopoulos et al., 2020b) could not be designed through CAMD due to the lack of group contribution data for all the necessary properties for the groups that they contain. For example, there are no data for calculation of critical properties of amides in (Hukkerikar et al., 2012b). DMETEG is an exception; it appears only once in the Pareto fronts of (Papadopoulos et al., 2020b) with R22 as the refrigerant, which is a chlorine-containing molecule that was not considered in the CAMD search as it has detrimental effects on the ozone layer and it is banned. DMETEG's lack of appearance in the designed molecules in combination with Acetaldehyde as a refrigerant is an indication that it may be of inferior performance compared to the proposed mixtures. D$_1$ is a structure that has similarities with DMETEG and is further quite similar (different only by two carbon atoms) to Diethylene glycol dimethyl ether (DEGDME) investigated as an absorbent in (Fatouh and Murthy, 1993; Yokozeki, 2005) with R22 as the

refrigerant. The similarity of D_1 with DEGDME and with DMETEG indicates that the use of multiple ether groups in an absorbent does not result in better performance than absorbents such as DMF and DMAC (which do not contain ether oxygens), included in the mixtures of (Papadopoulos et al., 2020b).

Figure 6 illustrates features of the designed mixtures, compared to the optimum mixtures from literature identified in (Papadopoulos et al., 2020b), which are not clearly shown in **Figure 5**. **Figure 6** shows the maximum cooling output that can be generated by the designed mixtures. It is noteworthy that $D_{11,1}$, i.e., Acetaldehyde-Methanediol, generates 57.9 RT with *COP* of 0.76 whereas NH_3-H_2O generates 56.17 RT with *COP* of 0.74. Furthermore, mixture Butane-Ethanol (D_{23}) selected by Tora (Tora, 2013) exhibited at best a *COP* of 0.44, generating 33.19 RT. The mixtures from literature (denoted with "M") enable higher cooling output, which is achieved with lower total mixture flowrates. The absorbent flowrates are much higher in the designed mixtures, whereas the refrigerant flowrates are similar. This indicates that Acetaldehyde is less miscible in the designed absorbents.

The performance of all mixtures against NH_3/H_2O in all indicators is illustrated in **Figure 7**. Practically all mixtures indicate lower pressures and higher distillate-to-feed ratios than NH_3/H_2O, which are desirable features. In some cases, the designed mixtures require lower amounts of refrigerant, whereas the number of separation stages required in the rectifier is higher. The difference is very small as NH_3/H_2O requires three stages, the designed mixtures require four stages and the literature mixtures require five stages (Papadopoulos et al., 2020b). $D_{11,1}$ exhibits approximately 3% higher *COP* and cooling output than NH_3/H_2O. $D_{15,1}$, and $D_{11,2}$ also exhibit *COP* and cooling output values close to NH_3/H_2O. Butane/Ethanol clearly exhibits inferior performance.

Figure 8 illustrates the performance compared to NH_3 of selected working fluids, considering their refrigerants and absorbents as individual components, in terms of safety, health and environmental impact properties. The results for MDOL and MOEAC are from the current work, whereas values for the other chemicals are adopted from (Papadopoulos et al., 2020b). It appears that both MDOL and MOEAC exhibit similar or better performance compared to the other absorbents (and refrigerants) in the safety properties. MDOL also exhibits better performance than the other chemicals in the health and the environmental properties, except for the bioconcentration factor. It is also worth noting that although Butane exhibits similar or better performance than Acetaldehyde in most of the properties, its soil sorption coefficient and bioconcentration factor are much worse.

CONCLUSION

This work presented a CAMD approach for the design of working fluid mixtures for ABR processes. Unlike previous works, the proposed approach employed a conceptual ABR process model in the course of CAMD which captured major operational driving forces pertaining to refrigeration output, ease of separation of the

mixture in the generator and solubility of refrigerant and absorber. The CAMD approach further generated simultaneously both refrigerant and absorbent molecular structures which were evaluated directly in terms of their ABR process performance in the course of CAMD in various indicators. The ABR process was designed and optimized specifically for each generated mixture, prior to identifying the optimum options in a multi-criteria sense.

The obtained results indicated Acetaldehyde and Butane as the best refrigerants, being in line with the findings of Tora (Tora, 2013). On the other hand, we identified 17 absorbents, with 14 of them being considered for the first time, while three of them were previously proposed by Tora (Tora, 2013). These absorbents were all combined into mixtures with both Acetaldehyde and Butane and evaluated in a multi-criteria methodology. Eventually, we identified the novel ABR mixtures Acetaldehyde/2-Methoxyethyl acetate and Acetaldehyde/Methanediol as the highest performing options. These mixtures were compared with NH_3/H_2O, indicating that Acetaldehyde/Methanediol exhibits 3% higher COP and cooling output than the reference mixture of NH_3/H_2O, and may also operate at 87 and 89% lower high and low cycle pressure. The novel mixtures were further compared with mixtures previously identified in (Papadopoulos et al., 2020b). Although in both cases the refrigerant is the same (Acetaldehyde), the absorbents are different, hence we find that the novel mixtures exhibit performance trade-offs in important indicators such as COP and exergy efficiency. For example, Acetaldehyde/Methanediol ($D_{11,1}$) exhibits 10.5% lower COP than Acetaldehyde/Methylpyrolidone (NMP-$M_{6,1}$), but it also exhibits 24% higher exergetic efficiency. However, the mixtures from (Papadopoulos et al., 2020b) indicate an overall better performance based on the aggregate index *J*. While the novel mixtures require similar refrigerant flowrates with the ones from (Papadopoulos et al., 2020b), they also require higher absorbent flowrates, whereas the number of separation stages in the rectifier is similar. These findings are justifiable, because the absorbents in the mixtures identified in (Papadopoulos et al., 2020b) include more complex (and apparently more efficient for ABR) functional groups which may not be used here due to the lack of group contribution data necessary to predict the properties of such structures during CAMD. The novel absorbent Methanediol further exhibits similar or better safety, health and environmental properties than NH_3. On the other hand, the proposed novel structures include similar groups to the ones contained in the structures previously proposed in (Tora, 2013). Although considered and identified by the CAMD approach, the mixtures designed in (Tora, 2013) are not identified in the Pareto fronts presented here, indicating that they exhibit suboptimal performance. Furthermore, the mixture eventually selected in (Tora, 2013) exhibits inferior performance to NH_3/H_2O, whereas our novel mixture of Acetaldehyde/Methanediol exhibits higher COP and cooling output. Finally, it is worth noting that through the proposed CAMD implementation, the results are obtained after evaluation of approximately 120,000 mixtures. This is only a very small fraction of the mixtures that would need to be evaluated in an exhaustive approach, as $2.2 * 10^6$ structures may be attained for

each one of the mixture components without considering their combination in different concentrations.

DATA AVAILABILITY STATEMENT

The original contributions presented in the study are included in the article/**Supplementary Material**, further inquiries can be directed to the corresponding author.

AUTHOR CONTRIBUTION

AIP: Software, Visualization, Conceptualization, Writing – Review and Editing, Supervision, Funding acquisition, AK: Software, Writing—Review and Editing, PS: Conceptualization, Writing—Review and Editing, Supervision, Funding acquisition, IH: Conceptualization, Writing—Review and Editing, Funding acquisition.

FUNDING

SUPPLEMENTARY MATERIAL

The Supplementary Material for this article can be found online at: https://www.frontiersin.org/articles/10.3389/fceng.2021.622998/full#supplementary-material.

REFERENCES

Achenie, L., Venkatasubramanian, V., and Gani, R. (2003). *Computer aided molecular design: theory and practice*. Amsterdam, Netherlands: Elsevier.

Adewusi, S. A., and Zubair, S. M. (2004). Second law based thermodynamic analysis of ammonia-water absorption systems. *Energy Convers. Manag.* 45, 2355–2369. doi:10.1016/j.enconman.2003.11.020

Ando, E., and Takeshita, I. (1984). Residential gas-fired absorption heat pump based on R 22-DEGDME pair. Part 1 thermodynamic properties of the R 22-DEGDME pair. *Int. J. Refrig.* 7, 181–185. doi:10.1016/0140-7007(84)90098-7

AspenTech (2019). AspenPlus Software. Available at: https://www.aspentech.com/ (Accessed November 2019).

Assael, M. J., Trusler, J. P. M., and Tsolakis, T. F. (1996). *Thermophysical properties of fluids: an Introduction to their prediction*. London, United Kingdom: Imperial College Press.

Austin, N. D., Sahinidis, N. V., and Trahan, D. W. (2017). A COSMO-based approach to computer-aided mixture design. *Chem. Eng. Sci.* 159, 93–105. doi:10.1016/j.ces.2016.05.025

Austin, N. D., Sahinidis, N. V., and Trahan, D. W. (2016a). Computer-aided molecular design: an introduction and review of tools, applications, and solution techniques. *Chem. Eng. Res. Des.* 116, 2–26. doi:10.1016/j.cherd.2016.10.014

Austin, N. D., Samudra, A. P., Sahinidis, N. V., and Trahan, D. W. (2016b). Mixture design using derivative-free optimization in the space of individual component properties. *Aiche J.* 62, 1514–1530. doi:10.1002/aic.15142

Azhar, M., and Siddiqui, M. A. (2019). Exergy analysis of single to triple effect lithium bromide-water vapour absorption cycles and optimization of the operating parameters. *Energ. Convers. Manag.* 180, 1225–1246. doi:10.1016/j.enconman.2018.11.062

Best, R., and Rivera, W. (2015). A review of thermal cooling systems. *Appl. Therm. Eng.* 75, 1162–1175. doi:10.1016/j.applthermaleng.2014.08.018

Buxton, A., Livingston, A. G., and Pistikopoulos, E. N. (1999). Optimal design of solvent blends for environmental impact minimization. *Aiche J.* 45, 817–843. doi:10.1002/aic.690450415

ChemSafetyPro (2019a). Bioconcentration factor 2019. Available at: https://www.chemsafetypro.com/Topics/CRA/Bioconcentration_Factor_BCF.html (Accessed November 2019).

ChemSafetyPro (2019b). Soil adsorption coefficient. Available at: https://www.chemsafetypro.com/Topics/CRA/Soil_Adso (Accessed November 2019).

Cignitti, S., Mansouri, S. S., Woodley, J. M., and Abildskov, J. (2018). Systematic optimization-based integrated chemical product-process design framework. *Ind. Eng. Chem. Res.* 57, 677–688. doi:10.1021/acs.iecr.7b04216

EPI suite (2019). EPI suite software 2019. Available at: https://www.epa.gov/tsca-screening-tools/epi-suitetm-estimation-program-interface (Accessed November 2019).

Fatouh, M., and Murthy, S. S. (1993). Comparison of R22-absorbent pairs for vapour absorption heat transformers based on P-T-X-H data. *Heat Recovery Syst. CHP* 13, 33–48. doi:10.1016/0890-4332(93)90023-O

Ghafoor, A., and Munir, A. (2015). Worldwide overview of solar thermal cooling technologies. *Renew. Sust. Energy Rev.* 43, 763–774. doi:10.1016/j.rser.2014.11.073

Gkouletsos, D., Papadopoulos, A. I., Seferlis, P., and Hassan, I. (2019). Systematic modeling under uncertainty of single, double and triple effect absorption refrigeration processes. *Energy* 183, 262–278. doi:10.1016/j.energy.2019.06.067

Hansen, C. M. (2004). 50 years with solubility parameters-past and future. *Prog. Org. Coat.* 51, 77–84. doi:10.1016/j.porgcoat.2004.05.004

Herold, K., Radermacher, R., and Klein, S. (2006). *Absorption chillers and heat pumps*. 2nd Edn.. Boca Raton, FL: CRC Press. doi:10.1201/b19625-14

Hukkerikar, A. S., Kalakul, S., Sarup, B., Young, D. M., Sin, G., and Gani, R. (2012a). Estimation of environment-related properties of chemicals for design of sustainable processes: development of group-contribution+ (GC+) property models and uncertainty analysis. *J. Chem. Inf. Model.* 52, 2823–2839. doi:10.1021/ci300350r

Hukkerikar, A. S., Sarup, B., Ten Kate, A., Abildskov, J., Sin, G., and Gani, R. (2012b). Group-contribution+ (GC+) based estimation of properties of pure components: improved property estimation and uncertainty analysis. *Fluid Phase Equilib.* 321, 25–43. doi:10.1016/j.fluid.2012.02.010

ICAS (2019). ICAS-DTU. Available at: https://www.kt.dtu.dk/english/research/kt-consortium/software (Accessed November 2019).

Jonuzaj, S., and Adjiman, C. S. (2017). Designing optimal mixtures using generalized disjunctive programming: hull relaxations. *Chem. Eng. Sci.* 159, 106–130. doi:10.1016/j.ces.2016.08.008

Jonuzaj, S., Akula, P. T., Kleniati, P. M., and Adjiman, C. S. (2016). The formulation of optimal mixtures with generalized disjunctive programming: a solvent design case study. *Aiche J.* 62, 1616–1633. doi:10.1002/aic.15122

Jonuzaj, S., Gupta, A., and Adjiman, C. S. (2018). The design of optimal mixtures from atom groups using generalized disjunctive programming. *Comput. Chem. Eng.* 116, 401–421. doi:10.1016/j.compchemeng.2018.01.016

Kale, P. L., Bothra, S. L., and Anklekar, R. M. (2018). Natural gas fired power plant with trigeneration of power, process heat and refrigeration using waste heat recovery. *Int. J. Sci. Eng. Res.* 9, 1188–1194.

Khamooshi, M., Parham, K., and Atikol, U. (2013). Overview of ionic liquids used as working fluids in absorption cycles. *Adv. Mech. Eng.* 5, 620592. doi:10.1155/2013/620592

Liu, Q., Zhang, L., Liu, L., Du, J., Tula, A. K., Eden, M., et al. (2019). OptCAMD: an optimization-based framework and tool for molecular and mixture product design. *Comput. Chem. Eng.* 124, 285–301. doi:10.1016/j.compchemeng.2019.01.006

Louaer, I., Meniai, A.-H., Larkeche, O., and Bencheikh-Lehocine, M. (2007). Computer-aided design and test of new refrigerants for anabsorption cycle

using group contribution methods. *Desalination* 206, 620–632. doi:10.1016/j.
desal.2006.04.067

Ng, L. Y., Andiappan, V., Chemmangattuvalappil, N. G., and Ng, D. K. S. (2015a).
A systematic methodology for optimal mixture design in an integrated
biorefinery. *Comput. Chem. Eng.* 81, 288–309. doi:10.1016/j.compchemeng.
2015.04.032

Ng, L. Y., Chong, F. K., and Chemmangattuvalappil, N. G. (2015b). Challenges and
opportunities in computer-aided molecular design. *Comput. Chem. Eng.* 81,
115–129. doi:10.1016/j.compchemeng.2015.03.009

Papadopoulos, A., Seferlis, P., and Hassan, I. (2020a). Working fluids for
absorption refrigeration processes, Patent No. 63,003/593.

Papadopoulos, A. I., Tsivintzelis, I., Seferlis, P., and Linke, P. (2018). "Computer-
aided molecular design: fundamentals, methods, and applications." in *Elsevier
reference module in chemistry, molecular sciences and chemical engineering*, Editor
J. Reedijk (Waltham, MA: Elsevier). doi:10.1016/B978-0-12-409547-2.14342-2

Papadopoulos, A. I., Gkouletsos, D., Champilomatis, V., Giannakakis, A., Kousidis,
V., Hassan, I., et al. (2020b). Systematic assessment of working fluid mixtures
for absorption refrigeration based on techno-economic, environmental, health
and safety performance. *Energy Convers. Manag.* 223, 113262. doi:10.1016/j.
enconman.2020.113262

Papadopoulos, A. I., Kyriakides, A.-S., Seferlis, P., and Hassan, I. (2019).
Absorption refrigeration processes with organic working fluid mixtures- A
review. *Renew. Sust Energy Rev.* 109, 239–270. doi:10.1016/j.rser.2019.04.016

Papadopoulos, A. I., and Linke, P. (2006). Multiobjective molecular design for
integrated process-solvent systems synthesis. *Aiche J.* 52, 1057–1070. doi:10.
1002/aic.10715

Papadopoulos, A. I., Stijepovic, M., Linke, P., Seferlis, P., and Voutetakis, S. (2013).
Toward optimum working fluid mixtures for organic rankine cycles using
molecular design and sensitivity analysis. *Ind. Eng. Chem. Res.* 52,
12116–12133. doi:10.1021/ie400968j

Reid, R. C., Prausnitz, J. M., and Poling, B. E. (1987). *The properties of gases and
liquids.* 4th Edn.. New York, NY: MacGraw-Hill.

Samudra, A. P., and Sahinidis, N. V. (2013). Optimization-based framework for
computer-aided molecular design. *Aiche J.* 59, 3686–3701. doi:10.1002/aic.14112

Shirazi, A., Taylor, R. A., Morrison, G. L., and White, S. D. (2018). Solar-powered
absorption chillers: a comprehensive and critical review. *Energy Convers.
Manag.* 171, 59–81. doi:10.1016/j.enconman.2018.05.091

Sinha, M., Achenie, L. E. K., and Gani, R. (2003). Blanket wash solvent blend design
using interval analysis. *Ind. Eng. Chem. Res.* 42, 516–527. doi:10.1021/ie020224l

Sun, J., Fu, L., and Zhang, S. (2012). A review of working fluids of absorption cycles.
Renew. Sust. Energ. Rev. 16, 1899–1906. doi:10.1016/j.rser.2012.01.011

Takeshita, I., Yamamoto, Y., Harada, T., and Wakamatsu, N. (1984). Residential
gas-fired absorption heat pump based on R22-DEGDME pair. Part 2 design,
computer simulation and testing of a prototype. *Int. J. Refrig.* 7, 313–321. doi:10.
1016/0140-7007(84)90121-X

Ten, J. Y., Hassim, M. H., Chemmangattuvalappil, N., and Ng, D. K. S. (2016). A
novel chemical product design framework with the integration of safety and
health aspects. *J. Loss Prev. Process Ind.* 40, 67–80. doi:10.1016/j.jlp.2015.
11.027

Tora, E. A. (2013). Computer-aided design and simulation of working fluid pairs
for absorption refrigerators. *Int. J. Sci. Eng. Res.* 4, 1306–1310.

Tyagi, K. P. (1983). Comparison of binary mixtures for vapour absorption
refrigeration systems. *J. Heat Recovery Syst.* 3, 421–429. doi:10.1016/0198-
7593(83)90057-7

Van Dyk, B., and Nieuwoudt, I. (2000). Design of solvents for extractive distillation.
Ind. Eng. Chem. Res. 39, 1423–1429. doi:10.1021/ie9904753

Wennberg, A. C., and Petersen, K. (2017). *Biodegradation of selected offshore
chemicals.* Oslo, Norway: NIVA.

Yokozeki, A. (2005). Theoretical performances of various refrigerant-absorbent
pairs in a vapor-absorption refrigeration cycle by the use of equations of state.
Appl. Energ. 80, 383–399. doi:10.1016/j.apenergy.2004.04.011

Zarogiannis, T., Papadopoulos, A. I., and Seferlis, P. (2016). Systematic selection of
amine mixtures as post-combustion CO_2 capture solvent candidates. *J. Clean.
Prod.* 136, 159–175. doi:10.1016/j.jclepro.2016.04.110

Zhang, L., Fung, K. Y., Wibowo, C., and Gani, R. (2018). Advances in
chemical product design. *Rev. Chem. Eng.* 34, 319–340. doi:10.1515/
revce-2016-0067

Zhang, L., Mao, H., Liu, Q., and Gani, R. (2020). Chemical product design-recent
advances and perspectives. *Curr. Opin. Chem. Eng.* 27, 22–34. doi:10.1016/j.
coche.2019.10.005

GLOSSARY

A_k^j Matrix indicating frequency of occurrence of each group in component j

c_I Mixture concentration

COP Coefficient of performance

D Vector of design parameters in CAMD optimization

d Design parameter with $d \in D$

D'_{opt} Pareto front obtained from **Eqs. 11–19**

ds Flowrate of stream exiting from the rectifier top

ds/f Distillate-to-feed ratio

$F_l(x, d)$ Performance indicator l used as objective functions in CAMD

f Flowrate of stream entering the generator

G_k Set of functional groups used in CAMD

J Aggregate index used for evaluation of mixtures

k Number of functional groups used in each iteration of CAMD

M_k^a First component of mixture in CAMD

"M_k^b" Second component of mixture in CAMD

$\dot{m}$ Mass flowrate (kg/s)

m_k^j Vector of functional groups in CAMD for component j

n_{ex} Exergy efficiency

N_{of} Number of objective functions

n^{stage} Number of stages in rectifier

P Pressure (Pa)

Q Heat load (kW)

T Temperature (K)

T_b Boiling point temperature

T_m Melting point temperature (K)

x State variables of the ABR model

y Vapor fraction

z_{ref} Mole fraction of refrigerant

Subscript/Superscripts

abs Absorber or absorbent

cnd Condenser

evp Evaporator

gen Generator

hex Heat exchanger

in Inlet stream

lim limit

out Outlet stream

ref Refrigerant

throt Throttle

Greek Abbreviations

δ_s Hansen solubility parameter (MPa)$^{0.5}$

ε_1 Upper limit for solubility of components

ε_2 Lower limit for boiling point temperature difference

ε_3 Upper melting point temperature limit for avoidance of solidification